This document is the Accepted Manuscript version of a Published Work that appeared in final form in ACS Sustainable Chem. Eng. 2016, 4, 2232−2242, © American Chemical Society after peer review and technical editing by the publisher. To access the final edited and published work see https://pubs.acs.org/doi/10.1021/acssuschemeng.5b01722

Fractionation of Industrial Softwood Kraft Lignin: Solvent Selection as a Tool for Tailored Material Properties

*Valeria Passoni, Carmela Scarica, Marinella Levi, Stefano Turri, and Gianmarco Griffini**

Department of Chemistry, Materials and Chemical Engineering "Giulio Natta", Politecnico di Milano, Piazza Leonardo da Vinci 32, 20133 Milano, Italy

ABSTRACT: A simple approach for the fractionation of industrial softwood kraft lignin is presented in this work aimed at predictively obtaining readily usable lignin fractions with tailored material properties in a straightforward manner. This method is based on the use of three distinct solvents of different chemical nature to isolate soluble and insoluble fractions from the parent lignin by a single-step extraction process. A thorough characterization of the soluble and insoluble lignin fractions highlighted a direct correlation between the chemical−physical characteristics of the extraction solvent and the final properties of the recovered materials. In particular, hydrogen bonding interactions between solvent and lignin were demonstrated to play a major role in the extraction process, controlling to a great extent the final materials properties. The results of this study give a clear demonstration of a straightforward approach to access easily lignin fractions with well-defined characteristics and provide strong evidence of the direct correlation between solvent characteristics and properties of the extracted materials as predictive tool for the development of high-performance lignin-based systems. KEYWORDS: Lignin, Fractionation, Thermal properties, Biobased, Polymer

Received: December 16, 2015
Revised: January 29, 2016
Published: February 19, 2016

INTRODUZIONE

The increasing global awareness toward environmental issues that has gained momentum in the past few decades together with the incumbent need of resorting to environmentally friendly primary resources for chemicals, materials and energy have propelled in the past few years the growth of the so-called sustainable development.[1] In this context, the biorefinery concept and related research and development efforts have become a concrete approach to tackle such key societal and technological challenges.[2] To date, most biorefineries are fed with lignocellulosic feedstock, the latter commonly consisting of agricultural wastes. Cellulose, hemicellulose, tannin and lignin constitute the main components of lignocellulosic biomass, in which they are present in varying proportions. In particular, lignin represents the most abundant terrestrial source of renewable aromatics and is currently produced at a rate of several million tons per year.[3−5]

Despite its great abundance, lignin is currently employed mainly as low-cost fuel for power and heat generation, with only a little fraction commercialized as additive, filler or dispersant in composites, binders or coatings.[6,7] Such a narrow spectrum of applications is largely attributable to the vast chemical, structural and compositional complexity and heterogeneity of the available lignins, which are greatly affected by the type of extraction process used to isolate them as well as by the type of lignocellulosic feedstock from which they are obtained. As a result, current lignins are characterized by highly variable and often very different properties that inevitably limit their straightforward usability. In this context, softwood kraft lignins represent an interesting class of lignocellulose materials as they are typically considered more uniform compared to the other different wood species as a result of their chemical structure, predominantly consisting of one single type of monolignol as building block (i.e., the guaiacyl-propane unit).[8] In particular, industrial softwood lignins are known to possess glass transition temperatures (T_g) in the 140−180 °C range, poor solubility in common solvents and wide distribution of molecular weights, making this material difficult to use for value-added applications such as the development of highly performing polymeric materials.[5,9−12]

To this end, different approaches have been developed in the past few years to overcome some of the above issues. Among these, chemical modification via methylation, esterification or benzylation reactions on the hydroxyl groups of lignin has been shown to allow the disruption of inter- and intrachain hydrogen bonds that are partially responsible for its brittleness, thus leading to a reduction of T_g.[13−16] A similar plasticization effect could also be accomplished by the use of appropriate additives (plasticizers), which are able to establish hydrogen bonds with the hydroxyl groups present in lignin and lead to a lower-T_g material.[17]

In the attempt to improve lignin miscibility in common solvents, to enhance its compatibility with other polymers and to gain access to more controlled chemical and structural properties, fractionation has been proposed as an efficient way to obtain lignin fractions with narrow molecular weight distribution, well-defined chemical composition and tunable chemical functionality. To date, three main fractionation approaches have been reported in the literature, namely selective precipitation at reduced pH values,[18−21] membrane-assisted ultrafiltration,[22,23] and extraction with solvent.[24−26]

Since the seminal works by Morck and co-workers,[27,28] successive solvent extraction has become one of the most widely employed techniques to isolate lignin fractions by sequentially processing the parent material with solvents of increasing hydrogen-bonding capability or increasing solubility parameters. This strategy has been used to treat lignins obtained from different pulping processes, with a major focus on the recovery of usable fractions from black liquors. However, although this method constitutes a valid platform to study the physical, chemical and functional properties of the resulting lignin fractions, it is not free from technological constraints that may result in prospective economic limitations on a large industrial scale. In particular, such an approach requires long and repeated extraction steps to obtain quantitative amounts of usable lignin for further processing, thus potentially resulting in increased material consumption and process costs.[29]

For the purpose of exploiting the full potential of lignin as building block for the development of new biobased polymeric materials, it is of great importance to develop a solvent fractionation methodology that allows to obtain readily usable lignin fractions with well-defined characteristics in a straightforward and economic fashion. In addition, particular emphasis should be given to the correlations between the chemical-physical characteristics of the solvents used for the extraction process and the chemical, physical and thermal properties of the extracted materials, which could potentially allow for a predictive screening of the resulting materials. Nevertheless, most of the works dealing with lignin fractionation via successive solvent extraction have mainly focused on the chemical characterization of the isolated lignin fractions, partly overlooking key aspects associated with the relationships between solvent and materials properties.

Herein, a simple fractionation approach is proposed and applied to a softwood commercially available technical lignin. Three distinct solvents of different chemical nature (namely an alcohol, a cyclic ether and a ketone) were separately employed to isolate soluble and insoluble fractions from the parent lignin by a single-step extraction process. These solvents were chosen because of their different nature, polarity and ability to form hydrogen bonds with lignin. All fractions recovered from each solvent treatment (both soluble and insoluble) were thoroughly characterized in terms of their chemical, physical, thermal and structural properties and a correlation between the properties of the solvent and the physical-chemical characteristics of the resulting fractions was proposed, that may allow to evaluate predictively the properties of the obtained materials. This aspect is of great importance when considering the possibility of selecting lignin fractions with tailored characteristics for target applications with specific material requirements (e.g., high T_g for use as building-blocks in epoxy-based materials, high molecular weight for use as filler in composite materials, low molecular weight for use as plasticizer, high phenolic hydroxyl content for use in phenol-formaldehyde resins, high thermal stability for use as carbon-fiber precursor).[30,31]

The results of this study give a clear demonstration of a straightforward approach to access easily lignin fractions with well-defined characteristics that can be efficiently exploited for the development of new biobased materials. In addition, this work provides a greater understanding of the relationships between solvent and materials properties, being this aspect of paramount importance for the development of highly performing lignin-based polymeric systems.

■ EXPERIMENTAL SECTION

Materials. The softwood kraft lignin used in this work (Indulin AT) was supplied by MeadWestvaco. All the solvents used for lignin solubilization (dimethyl sulfoxide) and for lignin fractionation (tetrahydrofuran, methanol and 2-butanone) were of analytical grade and were supplied by Sigma-Aldrich.

Lignin Fractionation and Extraction. Lignin samples were fractionated by means a Soxhlet apparatus. In brief, 4 g of lignin was added to 150 mL of each solvent in a round-bottomed flask equipped with the Soxhlet extractor. The temperature was raised 20 °C above the solvent boiling temperature (T_b = 66, 65 and 80 °C for tetrahydrofuran, methanol and 2-butanone, respectively) to obtain a constant reflux of liquid in the extraction chamber. The extraction process was allowed to proceed for 8 h under vigorous magnetic stirring. At the end of it, the insoluble fraction was collected while the solubilized lignin was recovered by rotary evaporation. Both fractions were dried in a vacuum-oven until constant weight was reached and the yield of the extraction process was then calculated by comparing the weight of the so-obtained soluble and insoluble dry fractions with the weight of the parent lignin material. Solubility tests with dimethyl sulfoxide on Indulin AT were performed at room temperature by magnetically stirring a 30 mg/mL lignin solution.

Materials Characterization. *Fourier Transform Infrared Spectroscopy (FTIR).* The FTIR spectra of all lignin fractions were recorded in transmission mode on films spin-cast onto KBr disks. The analysis was performed by means of a Nicolet 760-FTIR Spectrophotometer at room temperature in air in the 4000−700 cm^{-1} wavenumber range with 64 accumulated scans and a resolution of 2 cm^{-1}.

^{13}C NMR. Quantitative ^{13}C NMR spectroscopy was performed on acetylated samples to evaluate the amount of aliphatic and aromatic hydroxyl groups. Acetylation was performed following a procedure reported in the literature.[32] ^{13}C NMR analyses were carried out on a Bruker Avance 500 spectrometer in DMSO-d_6 and spectra were collected with a 200 ppm spectral width, 32 000 points of acquisition, a relaxation delay of 12 s and a 4 Hz line broadening. The chemical shifts of the peaks in the spectra were referenced to the chemical shift of DMSO-d_6 (δ = 39.5 ppm). The quantification of C atoms was performed by computing the following integration intervals: δ = 170.4−169.4 ppm for primary aliphatic hydroxyls OH(I), δ = 169.4−168.5 ppm for secondary aliphatic hydroxyls OH(II), δ = 168.5−165.8 ppm for phenolic hydroxyls OH(ϕ), δ = 160−100 ppm for aromatic carbons (that include oxygenated carbons C_{Ar-O} at δ = 160−142 ppm, nonoxygenated carbons C_{Ar-C} at δ = 142−125 ppm and protonated carbons C_{Ar-H} at δ = 125−100 ppm), δ = 90−58 ppm for aliphatic C−O and δ = 58−54 ppm for methoxy OCH_3.

UV−vis Absorption Spectroscopy. UV−vis absorption measurements were performed in air at room temperature in transmission mode by means of an Evolution 600 UV−vis Spectrophotometer (Thermo Scientific). Dimethyl sulfoxide (DMSO) was used as solvent for all samples.

Gel Permeation Chromatography (GPC). Gel permeation chromatography (GPC) was used to determine the molecular weight of lignin samples. A Waters 510 HPLC system was used equipped with a Waters 486 Tunable Absorbance Detector set at λ = 300 nm. THF was used as eluent. The sample to analyze (volume 200 μL,

Table 1. Hansen Solubility Parameter δ_{tot} (with Dispersive δ_d, Polar δ_p and Hydrogen Bonding δ_h components) and Molar Volume V_m for P-Lignin and the Solvents Employed in This Work[a]

	fractionation yield (%)	δ_d [(J/cm^3)$^{1/2}$]	δ_p [(J/cm^3)$^{1/2}$]	δ_h[(J/cm^3)$^{1/2}$]	δ_{tot} [(J/cm^3)$^{1/2}$]	V_M [(cm^3/mol)]	χ_{PS}
P-lignin[b]		16.7	13.7	11.7	24.6	2869.2	
dimethyl sulfoxide	>99[c]	18.4	16.4	10.2	26.7	71.3	0.70
tetrahydrofuran	62 ± 5	16.8	5.7	8.0	19.5	81.7	0.79
methanol	40 ± 5	15.1	12.3	22.3	29.6	40.7	1.97
2-butanone	21 ± 5	16.0	9.0	5.1	19.0	90.0	1.68

[a] The fractionation yield and the Flory–Huggins polymer–solvent interaction parameter χ_{PS} are also shown. [b] Data for P-lignin were obtained from ref 39. [c] Complete solubilization of P-lignin at room temperature.

concentration in THF 2 mg/mL) was injected into a system of columns connected in series (Ultrastyragel HR, Waters) and the analysis was performed at 30 °C and at a flow rate of 0.5 mL/min. The GPC system was calibrated against polystyrene standards in the 10^2–10^4 g/mol molecular weight range. To allow complete solubility in the THF eluent, the parent lignin and the soluble and insoluble fractions were acetylated before the analysis as previously described.[32]

Differential Scanning Calorimetry (DSC). Differential scanning calorimetry (DSC) was performed on solid state samples by means of a Mettler-Toledo DSC/823e instrument at a scan rate of 20 °C/min under nitrogen flux.

Thermogravimetric Analysis (TGA). Thermogravimetric analysis (TGA) was carried out on solid state samples with a Q500 TGA system (TA Instruments) from ambient temperature to 800 °C at a scan rate of 10 °C/min both in air and under nitrogen flux.

RESULTS AND DISCUSSION

Fractionation Yield and Solubility Model. To treat the parent softwood kraft lignin (Indulin AT, from here on referred to as P-lignin), a single-step extraction process was implemented consisting in the fractionation of P-lignin using a single solvent and then recovering the soluble and insoluble materials for further characterization. To this end, three distinct solvents were selected based on their different chemical nature, polarity and ability to form hydrogen bonds with lignin, namely tetrahydrofuran, methanol and 2-butanone. Solvent extraction of P-lignin was carried out in a Soxhlet apparatus for 8 h (see the Experimental Section for details) and a gravimetric assessment of the fractionation yield was performed. It was found that the highest extraction yield was obtained with tetrahydrofuran (62 ± 5%), followed by methanol (40 ± 5%) and 2-butanone (21 ± 5%) (Table 1). In the attempt to correlate these results with the thermodynamic miscibility of P-lignin in each investigated solvent, the Flory–Huggins polymer–solvent interaction parameter χ_{PS} was calculated for each solvent–lignin couple,[33,34] based on the approach introduced by Hildebrand and later extended by Hansen.[35,36] According to this theory, the solubility parameter δ_{tot} of a substance can be expressed as the sum of three contributions, namely dispersive (δ_d), polar (δ_p) and hydrogen bonding (δ_h), so that

$$\delta_{tot}^{\ 2} = \delta_d^{\ 2} + \delta_p^{\ 2} + \delta_h^{\ 2} \tag{1}$$

These terms come into play in the expression of χ_{PS}:[37]

$$\chi_{PS} = 0.34 + \frac{V_m}{RT}[(\delta_{dP} - \delta_{dS})^2 + (\delta_{pP} - \delta_{pS})^2 + (\delta_{hP} - \delta_{hS})^2] \tag{2}$$

where V_m is the molar volume of the solvent, R is the gas constant (8.314 J/(mol K)), T is the absolute temperature and the subscripts P and S stand for polymer and solvent, respectively.

Herein, calculations of the individual contributions to the solubility parameter of each solvent were based on the approach proposed by Hansen,[38] and the temperature employed in eq 2 was the boiling temperature of each solvent, as the lignin extraction process was conducted upon solvent reflux. The results of these calculations are presented in Table 1.

The different contributions (dispersive δ_d, polar δ_p and hydrogen bonding δ_h) to the solubility parameter of P-lignin show relatively comparable values, thus indicating that they all affect to a similar extent the resulting total solubility parameter of P-lignin (δ_{tot} = 24.6 (J/cm^3)$^{1/2}$). This behavior may be correlated with the complex chemical nature of P-lignin in which aromatic, aliphatic, carbonyl and hydroxyl groups can all give rise to different intermolecular interactions of reasonably comparable magnitude. The ability to establish such intermolecular interactions influences the solubility of P-lignin in a given solvent. To evaluate this effect, the Flory–Huggins interaction parameter for the P-lignin/dimethyl sulfoxide couple was calculated. Because dimethyl sulfoxide is normally found to be a good solvent for softwood kraft lignin (it can in fact be produced starting from kraft lignin)[40] as also observed in the present work (solubility > 99% at room temperature), the χ_{PS} value obtained for the P-lignin/dimethyl sulfoxide (χ_{PS} = 0.70) system may act as reference as it theoretically represents the maximum allowable value to achieve complete dissolution of P-lignin, in accordance with the Flory–Huggins theory. Positive deviations from this value should theoretically lead to a progressively poorer solubilization of P-lignin by the given solvent. As shown in Table 1, all solvents employed in this work exhibit χ_{PS} values higher than that found for dimethyl sulfoxide, in agreement with the lower (<99%) fractionation yields reported. In particular, tetrahydrofuran was found to exhibit the lowest χ_{PS} (0.79), well correlating with the fractionation yield obtained for this solvent. As opposed to this, 2-butanone and methanol possess significantly higher χ_{PS} values (1.68 and 1.97, respectively) and lead to correspondingly lower fractionation yields (20% and 40%, respectively). It is interesting to note that in the case of 2-butanone and methanol, a direct correlation between χ_{PS} and fractionation yield is not observed. In particular, a lower χ_{PS} is found in 2-butanone than in methanol, despite its lower fractionation yield. This behavior may be ascribed to the different contributions given to the solubility parameter by hydrogen bonding (δ_h) observed in these two solvents, namely 22.3 and 5.1 (J/cm^3)$^{1/2}$ for methanol and 2-butanone, respectively. Such 4-fold difference in δ_h may be responsible for a larger lignin extraction yield when methanol is employed, due to the higher ability of this solvent to establish easily hydrogen bonding interactions with

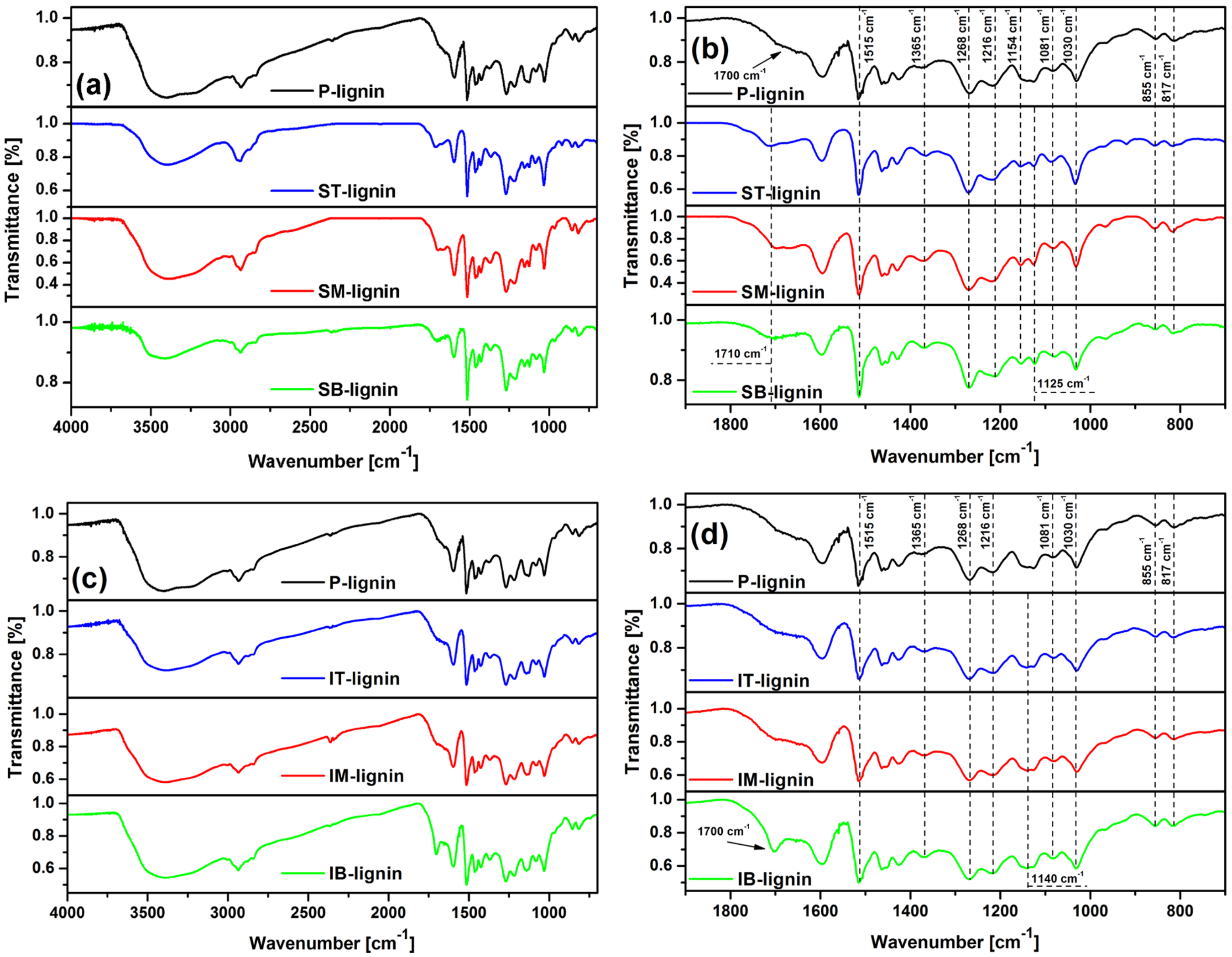

Figure 1. FTIR spectra of recovered soluble (a) and insoluble (c) lignin fractions, with enlarged views of the corresponding fingerprint regions (b and d). Materials obtained after treatment with tetrahydrofuran (T), methanol (M) and 2-butanone (B) are reported. For reference, the FTIR spectrum of the parent material (P-lignin) is also reported.

P-lignin, the latter being highly receptive to hydrogen bonds due to the abundance of hydroxyl and carbonyl groups present in its structure.

Fourier-Transform Infrared Spectroscopy (FTIR). To clarify better the nature of the interactions between parent lignin and fractionating solvent and to gain further insights into the chemical composition of each resulting lignin fraction, FTIR spectra were collected on all soluble and insoluble materials recovered upon treatment of P-lignin with each of the solvents examined in this work. For easy reference, all fractions will be denoted throughout the text with the acronyms SX (for soluble materials) or IX (for insoluble materials), with X being a letter indicating the solvent from which that specific fraction was recovered, namely tetrahydrofuran (T), methanol (M) or 2-butanone (B). FTIR spectra of all lignin systems are presented in Figure 1, where the FTIR spectrum of the parent P-lignin is also shown to allow for comparisons.

All fractions present a broad absorption band centered at 3390 cm^{-1} of variable intensity that can be attributed to stretching vibrations of phenolic and aliphatic O−H groups present in lignin. Similarly, four distinct signals are reported in the 3050−2800 cm^{-1} spectral region that are typically assigned to C—H stretching vibrations in methyl and methylene groups. Stretching vibrations of C═O bonds are typically found between 1740 and 1700 cm^{-1}. In particular, signals attributable to C═O bonds in unconjugated ketones, carbonyls and ester groups are normally observed in the 1740−1710 cm^{-1} region, while lower absorption energies (around 1700 cm^{-1}) are reported for conjugated aldehydes and carboxyl acids.[41] In this broad spectral region, P-lignin only shows a weak shoulder, thus indicating a relatively low concentration of C═O moieties and likely indicating relatively high purity of the starting material with low concentration of residual carbohydrate species. As opposed to this, the appearance of a peak at around 1710 cm^{-1} is clearly noticeable in all soluble fractions, suggesting that solvent extraction leads to increased concentration of carbonyl and carboxyl groups compared to P-lignin likely resulting from hydrogen bond interactions between extracting solvents and lignin. Accordingly, no notable signals in the 1740−1710 cm^{-1} spectral region are observed in the insoluble fractions. It is interesting to note that in the FTIR spectrum of IB-lignin a sharp peak centered at 1700 cm^{-1} (C═O stretching in conjugated aldehydes and carboxylic acids) is found. Conversely, only a weak signal (shoulder) is observed in IT- and IM-lignin fractions. This evidence well agrees with the lower hydrogen bonding capability of 2-butanone with respect to tetrahydrofuran and methanol (Table 1), that determines a higher concentration of carbonyl and carboxyl groups in the recovered insoluble material IB-lignin compared to IT- and IM-lignin. All spectra (soluble and insoluble fractions) are characterized by the presence of an intense peak at 1515 cm^{-1} that is typical of pure aromatic skeletal vibrations in lignin.[41] Vibrations associated with phenolic O—H groups are observed in the 1365−1370 cm^{-1} region, where also stretching vibrations of aliphatic C—H in methyl groups are seen. In the 1200−1300 cm^{-1} region, two peaks are found in all fractions centered at 1268 and 1216 cm^{-1} attributable to the presence of guaiacyl (G) moieties as they are normally associated with C—O vibrations in the G aromatic ring combined with C═O stretching, and to C—C, C—O and C═O stretching vibrations, respectively. All soluble fractions exhibit a clear peak at 1154 cm^{-1} that can be assigned to C═O deformations in conjugated ester groups present in G/syringyl (S)/*p*-hydroxyphenyl (H) lignins. Such a peak is only a weak shoulder in P-lignin, indicating that only a relatively small concentration of S and H moieties is present in the parent material. This evidence is further supported by the absence in P-lignin as well as in all fractions of signals at 835 cm^{-1}, which are typically assigned to C—H out-of-plane deformations in S and H units. Conversely, all fractions present clearly distinguishable peaks at 855 and 817 cm^{-1}, assigned to C—H out-of-plane deformations in G units. Similarly, a higher concentration of S units is found in the soluble fractions, as evidenced by the presence of a peak centered at 1125 cm^{-1} (C—H in plane deformation in S units) that is not observed in the insoluble materials. In the same region, all insoluble fractions are characterized by the appearance of a broad peak centered at 1140 cm^{-1}, which is typical of C—H aromatic in-plane deformations in G units. Signals associated with C—O deformations in primary (1030 cm^{-1}) and secondary (1081 cm^{-1}) alcohols are observed in all fractions, although with different relative intensities.

A semiquantitative determination of the relative abundance of −OH groups (aliphatic and aromatic) in the different fractions was carried out considering the signal centered at 1515 cm^{-1} present in all FTIR spectra (pure aromatic skeletal vibrations in lignin) as invariant band in each spectrum. In particular, the relative intensities of the peaks (with respect to the 1515 cm^{-1} peak) found at 3390 cm^{-1} (−OH stretching), 1365 cm^{-1} (phenolic −OH), 1081 cm^{-1} (aliphatic secondary −OH) and 1030 cm^{-1} (aliphatic primary −OH) were calculated and the results are presented in Table 2, where also values for P-lignin are reported.

The intensity of the peak related to the −OH stretching vibration (3390 cm^{-1}, phenolic and aliphatic hydroxyls) was found to be highest in SM-lignin, followed by ST- and SB-lignin. This result suggests that a higher concentration of hydroxyl groups is present in the methanol-soluble fraction compared to tetrahydrofuran and 2-butanone. A similar trend was observed for the FTIR signals ascribed to aliphatic (1030 and 1081 cm^{-1}) and phenolic (1365 cm^{-1}) −OH groups, with SM-lignin showing the highest peak intensity followed by ST- and SB-lignin (notwithstanding the multiple contributions given to these peaks from different vibrational modes).

These results may be explained by considering that methanol possesses a stronger ability to form hydrogen bonds with the hydroxyl groups present in P-lignin, as evidenced by the much higher hydrogen bonding component of its solubility parameter (δ_h) as compared to tetrahydrofuran and 2-butanone. As a result, a higher concentration of hydroxyls are expected to be conveyed into the methanol-soluble lignin fraction. Among the insoluble materials, IB-lignin presents the highest intensity for signals related to −OH, fully in agreement with the lowest peak intensity found in the soluble SB-lignin counterpart in the same spectral region. This trend well correlates with the relatively poor solubility of P-lignin in 2-butanone that results from the limited ability of this solvent to establish hydrogen bonds with the parent material. Because the poor solubility of lignin is largely attributed to the presence of strong hydrogen bonds between the hydroxyl groups in its molecular structure, limited affinity with the extracting solvent leads to a higher concentration of hydroxyls in its insoluble fraction.

Table 2. Relative Intensities[a] of FTIR Signals Associated to −OH Groups (Aliphatic Primary OH(I), Aliphatic Secondary OH(II) and Phenolic OH(ϕ)) in all Lignin Fractions (Soluble and Insoluble) Examined in This Work[b]

	OH (3390 cm^{-1})	OH(ϕ) (1365 cm^{-1})	OH(II) (1081 cm^{-1})	OH(I) (1030 cm^{-1})
P-lignin	0.91	0.07	0.10	0.54
ST-lignin	0.57	0.11	0.11	0.55
SM-lignin	0.74	0.14	0.12	0.60
SB-lignin	0.42	0.09	0.08	0.38
IT-lignin	0.82	0.09	0.09	0.51
IM-lignin	0.91	0.09	0.10	0.47
IB-lignin	0.99	0.13	0.12	0.54

[a] Calculations were performed normalizing the intensity of each peak with respect to the intensity of the signal at 1515 cm^{-1} in each FTIR spectrum considered as invariant band. [b] For comparison, data for P-lignin are also presented.

^{13}C NMR. In view of the use of lignin as a precursor for high-value-added polymeric materials, a quantification of the amount of hydroxyl groups in the parent material is required together with the evaluation of the effects of solvent treatment on the distribution of such functionalities in the different soluble and insoluble fractions. To this end, quantitative ^{13}C NMR analysis was performed on the parent material as well as on all lignin fractions, following a methodology previously published in the literature.[42]

As reported in Table 3, an overall decrease of the aliphatic (primary and secondary) hydroxyl group content compared to the parent P-lignin is observed in all solvent-extracted soluble fractions. In particular, the lowest concentration of both OH(I) and OH(II) is found in SB-lignin, with 0.22/Ar and 0.17/Ar, respectively. Conversely, the phenolic hydroxyl concentration is found to increase slightly in all soluble fractions (0.67/Ar, 0.70/Ar and 0.66/Ar for ST-, SM- and SB-lignin, respectively) in comparison with the parent material (0.61/Ar). These variations in the aliphatic and phenolic hydroxyl content yield an overall decrease of OH groups in all solvent-extracted soluble materials after solvent treatment of P-lignin. In this respect, SM-lignin (methanol soluble) shows the highest −OH group concentration (1.16/Ar) among the soluble fractions, followed by ST-lignin (1.15/Ar) and SB-lignin (1.05/Ar). In accordance with the results obtained from FTIR analysis, this behavior may be explained by considering the stronger ability of methanol to establish hydrogen bonds with OH groups in lignin than in the case of tetrahydrofuran and 2-butanone (large differences in δ_h). As a result, a lignin fraction with an overall larger amount of hydroxyls can be solubilized with methanol than with the other solvents. The lowest concentration of OH

Table 3. Relative Abundance of the Main Functional Groups and Linkages Expressed as Number of Associated Carbon Atoms per Aromatic Ring (Ar) for All Lignin Fractions Examined in This Work, As Obtained from ^{13}C-NMR Spectroscopy[a]

	OH(I)	OH(II)	OH(ϕ)	OH(tot)	C_{Ar-O}	C_{Ar-C}	C_{Ar-H}	aliphatic C−O	OCH_3
P-lignin	0.33	0.24	0.61	1.18	1.33	2.34	2.33	0.53	0.74
ST-lignin	0.28	0.20	0.67	1.15	1.38	2.35	2.27	0.52	0.85
SM-lignin	0.27	0.19	0.70	1.16	1.25	2.42	2.33	0.48	0.81
SB-lignin	0.22	0.17	0.66	1.05	1.28	2.45	2.27	0.27	0.74
IT-lignin	0.39	0.30	0.69	1.38	1.45	2.39	2.16	0.78	0.88
IM-lignin	0.42	0.31	0.57	1.30	1.49	2.42	2.09	0.96	0.82
IB-lignin	0.36	0.27	0.70	1.33	1.35	2.43	2.22	0.84	0.82

[a] For comparison, data for the parent material (P-lignin) are also presented.

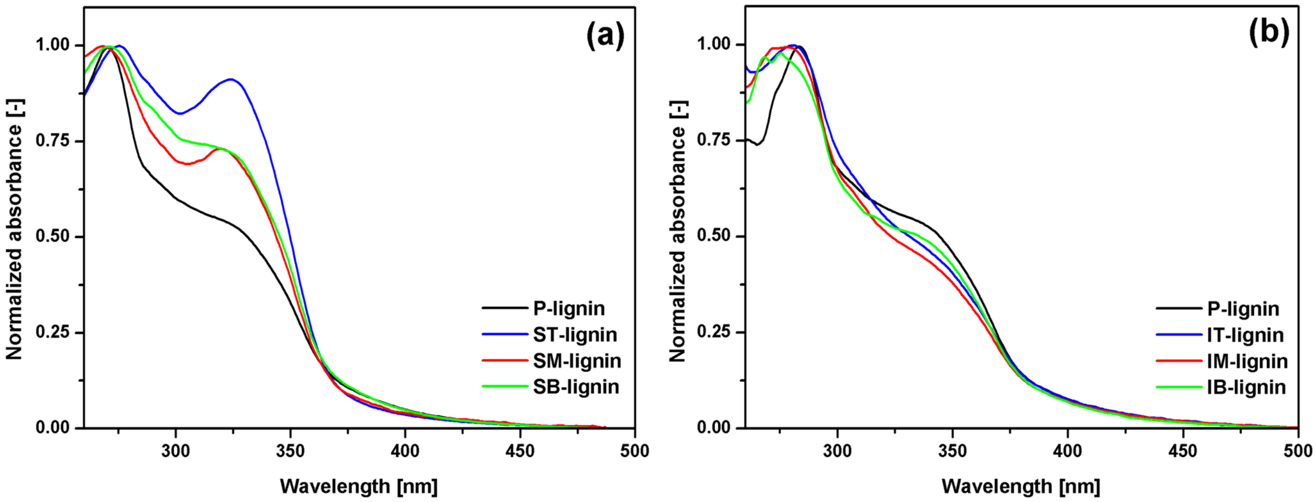

Figure 2. Normalized UV−vis spectra of recovered (a) soluble and (b) insoluble lignin fractions. Materials obtained after treatment with tetrahydrofuran (T), methanol (M) and 2-butanone (B) are reported. For reference, the UV−vis spectrum of the parent material (P-lignin) is also reported.

groups is found in SB-lignin, fully in agreement with the limited hydrogen bonding ability of 2-butanone. Consistent trends are also found in the insoluble materials, where the insoluble fraction recovered after methanol extraction (IM-lignin) presents the lowest concentration of total hydroxyls (1.30/Ar), as opposed to IT-lignin (1.38/Ar) and IB-lignin (1.33/Ar). In particular, it is worth noticing that all insoluble fractions present higher OH-group concentrations than the corresponding soluble counterparts, regardless of the solvent employed for extraction. The overall trends observed on the relative abundance of OH groups in the different lignin fractions as obtained from ^{13}C NMR analysis are in good agreement with those observed from the FTIR analysis presented earlier and further highlight the key role played in lignin solubility by the hydrogen bonding interactions between the hydroxyl groups present in its molecular structure.

To gain deeper knowledge of the modifications in the chemical structure of the treated lignin samples upon fractionation, an additional analysis of the relative abundance of the main functional groups and linkages was performed. As shown in Table 3, the amount of oxygenated aromatic carbon atoms (C_{Ar-O}) is found to be higher in all insoluble fractions compared to the corresponding soluble materials and P-lignin, irrespective of the solvent employed. This may indicate that solvent treatment leads to the partial rupture of aryl ether linkages present in the structure of the parent material, thus resulting in a higher relative abundance of such moieties in the insoluble fractions. A similar trend is observed on aliphatic C−O and methoxy OCH_3. As opposed to this, a slight decrease of protonated aromatic carbons (C_{Ar-H}) is reported in all insoluble fractions compared to the corresponding soluble counterparts, likely suggesting a higher degree of condensation in these materials (lower number of free positions in the aromatic ring).[19] Finally, no significant differences between soluble and insoluble fractions are found in the number of nonoxygenated aromatic carbon atoms (C_{Ar-C}). It is worth noticing that no signals were observed in the 100−90 ppm region, thus suggesting negligible carbohydrate content in these materials, in accordance with recent literature reports (Supporting Information).[43]

UV−vis Spectroscopy. UV−vis spectroscopy was used to evaluate qualitatively the effect of solvent treatment on the composition of the recovered lignin fractions. In particular, lignin absorption in the UV−vis region is mainly related to its highly aromatic structure, frequently conjugated with aliphatic double bonds and carbonyls.[44] Therefore, changes in the type and amount of conjugated moieties in lignin may result in observable modifications of the UV−vis absorption spectrum. Figure 2 presents the UV−vis spectra of all soluble and insoluble materials together with the reference P-lignin. In this work, UV−vis measurements were carried out dissolving each lignin fraction in dimethyl sulfoxide that allowed complete solubilization of the materials while limiting the absorption spectral range to wavelengths longer than 260 nm.

All lignins (soluble and insoluble fractions) present a maximum absorption peak at 270 nm that can be attributed

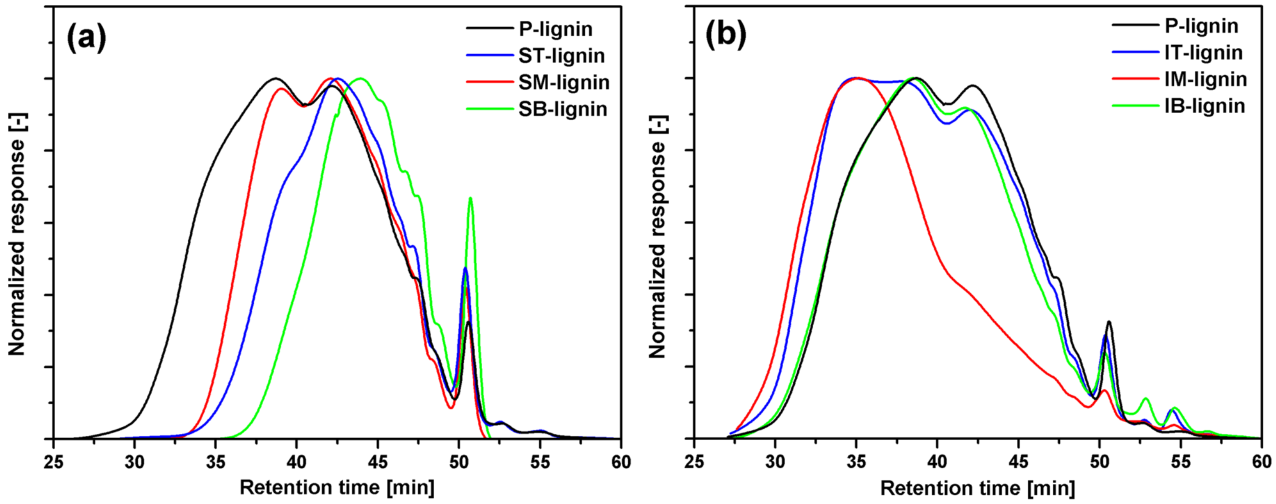

Figure 3. GPC chromatograms of recovered (a) soluble and (b) insoluble lignin fractions. Materials obtained after treatment with tetrahydrofuran (T), methanol (M) and 2-butanone (B) are reported. For reference, the GPC chromatogram of the parent material (P-lignin) is also reported.

to noncondensed phenolic groups in the guaiacyl unit.[25] Compared with the parent material, all soluble fractions also exhibit an additional absorption feature centered at 340 nm that can be ascribed to conjugated moieties such as α-carbonyl groups and esters of hydrocinnamic acids (e.g., ferulic acid) that are easily dissolved by the solvents used in this work.[45] In particular, a well-defined peak is observed in ST- and SM-lignin whereas a shoulder is found in SB-lignin. This peak shows its maximum intensity in ST-lignin, likely indicating that tetrahydrofuran allows one to solubilize better such conjugated species responsible for this absorption feature. On the other hand, the UV—vis spectra of all insoluble fractions are not found to differ significantly from the absorption spectrum of P-lignin, clearly indicating a significantly lower concentration of more conjugated species in the recovered insoluble material.

Gel Permeation Chromatography (GPC). GPC analysis was employed to elucidate the effect of solvent fractionation on the molecular weight distribution of all lignin fractions. Owing to the limited solubility in the GPC eluent (THF) of most of the materials recovered after solvent extraction, all lignin samples were acetylated prior to analysis to allow for consistent comparisons. Figure 3 reports the GPC chromatograms of all soluble and insoluble fractions as well as of the parent material.

The parent lignin material presents a broad molecular weight distribution with a partially bimodal profile. On the other hand, all recovered soluble fractions show narrower molecular weight distributions and longer retention times (t_R). Among these, SM-lignin (methanol soluble fraction) is found to exhibit the broadest molecular weight distribution with a significant contribution given by high-molecular-weight fractions (t_R < 40 min), whereas SB-lignin (2-butanone soluble fraction) is characterized by lower molecular weights (higher t_R values). A higher relative intensity of the low-molecular-weight peak (t_R = 51 min) is observed in SB-lignin compared to ST- and SM-lignin fractions, clearly indicating that 2-butanone allows one to extract a higher amount of low molecular weight species than the other solvents, in addition to yielding a narrower molecular weight distribution. Such low molecular weight fractions are generally oligomers and chain fragments that are not generated by the fractionation process but are already present in the parent material and increase their concentration in the soluble fraction upon solvent treatment.[43] Because of their relatively low hydroxyl group content,[46] they can be easily solubilized also by solvents with limited hydrogen bonding capability, as opposed to the higher molecular weight fractions. Along these lines, lower molecular weights and narrower molecular weight distributions could be obtained after fractionation with 2-butanone (M_n = 1100 g/mol and PDI = 1.5 for SB-lignin) as compared to the other solvents (M_n = 1360 g/mol and PDI = 1.7 for ST-lignin, M_n = 1610 g/mol and PDI = 1.8 for SM-lignin), as reported in Table 4. The high molecular weight and broad molecular weight distribution characterizing SM-lignin may be explained by considering the stronger ability of methanol to establish hydrogen bonds with the hydroxyl groups in lignin (high δ_h value), allowing for a larger portion of longer OH-rich macromolecular chains to be extracted upon solvent treatment compared to the other solvents. These results well correlate with the trends observed with FTIR (Figure 1) and ^{13}C NMR (Table 3) analyses. As to the insoluble fractions, they all present significantly higher molecular weights and PDI values compared to the corresponding soluble counterparts, with a markedly reduced contribution from the low molecular weight species eluting at t_R = 51 min. This behavior may indicate that the longer the macromolecular chains, the more difficult for the solubilizing solvent to penetrate their highly branched 3D structure. Such a hindrance effect may be

Table 4. Molecular Weights (M_n and M_w), Polydispersity Index (PDI), High Molecular Weight (HMW, t_R < 49 min) and Low Molecular Weight (LMW, t_R > 49 min) Areas of All Lignin Fractions (Soluble and Insoluble) Examined in This Work[a]

	M_n (g/mol)	M_w (g/mol)	PDI	HMW (%)	LMW (%)
P-lignin	1980	4680	2.4	98.4	1.6
ST-lignin	1360	2300	1.7	96.0	4.0
SM-lignin	1610	2910	1.8	97.0	3.0
SB-lignin	1100	1680	1.5	93.0	7.0
IT-lignin	2310	6010	2.6	99.8	0.2
IM-lignin	3500	8390	2.4	99.4	0.6
IB-lignin	2280	5080	2.2	99.0	1.0

[a] For comparison, data for the parent material (P-lignin) are also presented.

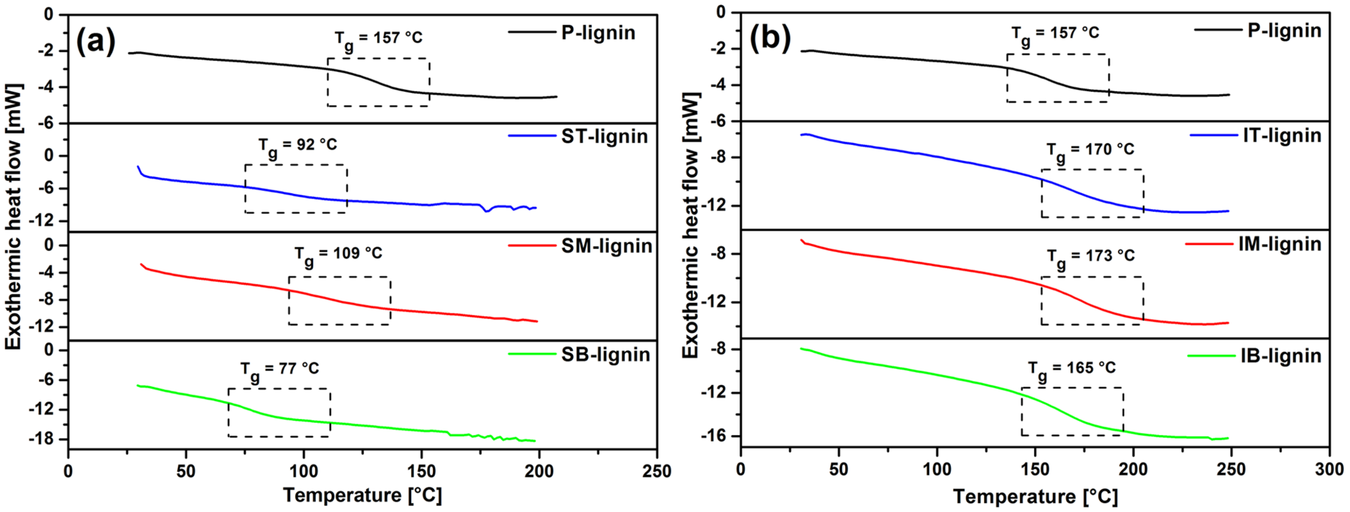

Figure 4. DSC traces of recovered (a) soluble and (b) insoluble lignin fractions. Materials obtained after treatment with tetrahydrofuran (T), methanol (M) and 2-butanone (B) are reported. For reference, the DSC trace of the parent material (P-lignin) is also reported.

responsible for limited chemical interactions between hydroxyls and solvent that are largely responsible for lignin solubilization. This phenomenon affects progressively longer macromolecules as the hydrogen bonding ability of the solvent increases. As a result, the insoluble material recovered from methanol fractionation (IM-lignin) exhibits a molecular weight distribution shifted toward significantly lower t_R values as compared to what found for the other solvents, and only very long highly branched macromolecular chains can be recovered from its insoluble fraction.

Differential Scanning Calorimetry (DSC). To investigate the effect of solvent treatment on the thermal properties of the recovered lignin fractions, DSC analysis was performed on all soluble and insoluble materials, and the results are presented in Figure 4, where the DSC trace for P-lignin is also reported for reference. All soluble fractions present significantly lower T_g values compared to P-lignin, clearly indicating that solvent fractionation represents an efficient and convenient way to obtain lower T_g systems without the need of chemical treatments on the parent material. More specifically, the methanol soluble fraction (SM-lignin) is found to give the highest T_g value (109 °C), followed by ST- (92 °C) and SB-lignin (77 °C). Conversely, all insoluble fractions exhibit T_g values substantially higher than the parent material. Also in this case, the insoluble fraction recovered after treatment with methanol (IM-lignin) is characterized by the highest T_g value (173 °C), whereas slightly lower T_g values are obtained for IT- (170 °C) and IB-lignin (165 °C).

These trends can be related to the different molecular weights of the lignin fractions as obtained from GPC analysis. In particular, for higher molecular weight fractions, a higher T_g value is expected. In the attempt to systematically investigate the correlation between T_g and molecular weight of each (soluble and insoluble) fraction, the Flory−Fox model was used:[47]

$$T_g = T_g^{\infty} - \frac{K}{M_n} \tag{3}$$

in which T_g^{∞} is the glass transition temperature of a polymer with high molecular weight in which the effect of chain ends is negligible, M_n is the number-average molecular weight and K is an empirical constant that can be correlated to the free volume of the material through the following expression:

$$K = \frac{2\vartheta N_A \rho}{\Delta\alpha_f} \tag{4}$$

with ϑ being the excess free volume of macromolecular chain ends, N_A the Avogadro's number, ρ the density of the material and $\Delta\alpha_f$ the free volume thermal expansion coefficient. Despite the uncertainties associated with the evaluation of the molecular weight by GPC analysis (which gives relative values for M_n and M_w) and the variability of the chemical composition among different lignin fractions (as evidenced by FTIR analysis), eq 3 may provide interesting qualitative information on the correlation between excess free volume and molecular weight of the lignin samples.

Figure 5 presents a plot of the T_g values of soluble and insoluble fractions as a function of the reciprocal of M_n. By linearly fitting the experimental data with the Fox−Flory equation, numerical values for K and T_g^{∞} could be estimated.

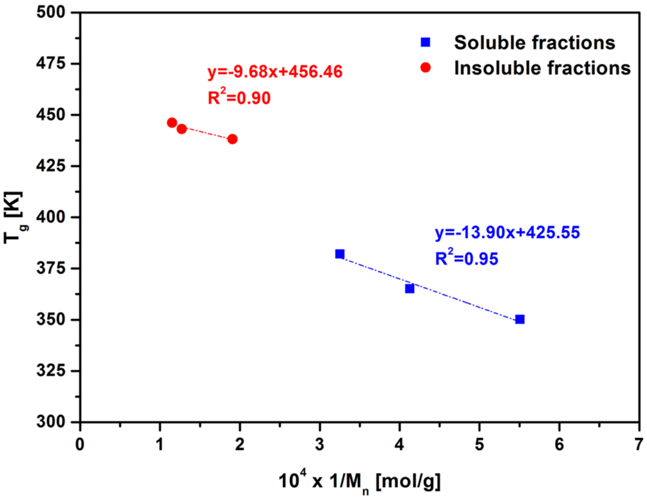

Figure 5. T_g of soluble and insoluble fractions as a function of M_n. The experimental data were fitted on the basis of the Flory−Fox model and the equations for the fitting curves are also reported.

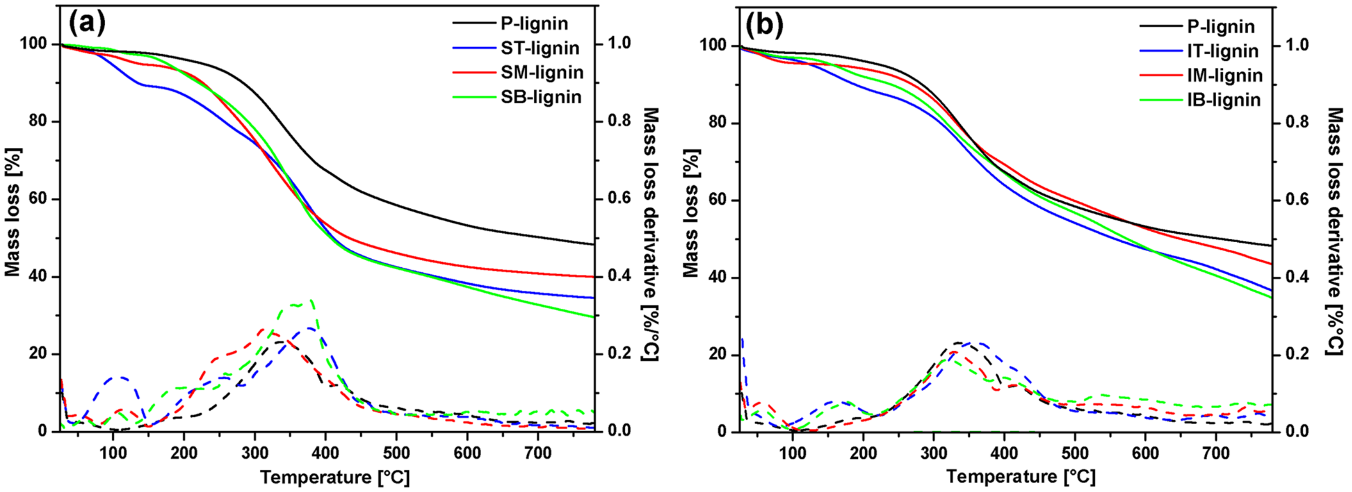

Figure 6. TGA curves in N_2 flux of recovered (a) soluble and (b) insoluble lignin fractions. Materials obtained after treatment with tetrahydrofuran (T), methanol (M) and 2-butanone (B) are reported. For reference, the TGA curve of the parent material (P-lignin) is also reported.

As indicated by the fitting equations reported in Figure 5, K values of 13.90 and 9.68 were calculated for the soluble and insoluble fractions, respectively. Assuming ρ and $\Delta\alpha_f$ to be constant for all materials, the obtained K values can be directly correlated with the excess free volume of the chain ends. Therefore, the higher value of K found for the soluble materials indicates that a larger excess free volume of chain ends is present in this case compared to the insoluble counterparts, which is partially responsible for the observed decrease of T_g (Figure 4). This behavior can also be correlated with the lower −OH group content found in the lignin soluble fractions compared to the corresponding insoluble counterparts (Table 2 and Table 3, FTIR and ^{13}C NMR), as the presence of polar groups such as hydroxyls is known to reduce the mobility of the macromolecular chains (and their free volume) thus leading to increased T_g.

It is interesting to note that the estimated values of T_g^{∞} obtained from the linear fit (426 and 457 K for the soluble and insoluble fractions, respectively) are comparable with the actual T_g measured for the reference P-lignin material by DSC analysis (430 K), thus suggesting the relatively minor role played by the chain ends in the highly branched three-dimensional structure of the parent lignin material.

Thermogravimetric Analysis (TGA). To investigate the effect of solvent fractionation on the thermal properties of the soluble and insoluble lignin fractions, TGA measurements were performed under N_2 and the results are presented in Figure 6 and Table 5.

After fractionation a decrease of thermal stability in all soluble fractions is observed compared to P-lignin, which is in line with the molecular weight reduction experienced by these materials upon fractionation (Figure 3 and Table 4). In particular, the temperature at which 10% weight loss occurs ($T_{10\%}$) is found to decrease significantly upon solvent treatment irrespective of the solvent used. Similarly, 50% of the mass loss occurs at markedly lower temperatures than the parent material. The higher mass loss observed in ST-lignin peaked at 100 °C may be ascribed to a larger amount of water and solvent trapped in this material as compared to the other soluble systems. Interestingly, ST-lignin also exhibits the largest maximum mass loss derivative temperature (T_{DTGmax}), clearly highlighting the high thermal stability of this material at high temperatures. The thermal stability is found to increase in all insoluble fractions, with a mass loss profile comparable with that observed on the parent material. The thermo-oxidative behavior of lignin fractions was examined by means of TGA under air flux (Supporting Information). A lower thermal stability of soluble materials in air was observed compared to P-lignin at temperatures lower than 400 °C, with ST-lignin undergoing the most significant mass loss event ($T_{10\%}$ = 142 °C). By increasing the temperature (T > 400 °C), all soluble fractions were found to exhibit similar thermo-degradative profiles, with 50% mass loss temperatures in the 470−480 °C range. Finally, all insoluble fractions showed a thermo-oxidative degradation behavior comparable to that found in the parent material, with $T_{10\%}$ values higher than the corresponding soluble counterparts.

Table 5. Thermal Degradation Temperatures at 10% ($T_{10\%}$) and 50% ($T_{50\%}$) Mass Loss, Final Char Residue at 780 °C (R_{780}) and Maximum Mass Loss Derivative Temperature (T_{DTGmax}) for All Lignin Fractions (Soluble and Insoluble) Examined in This Work, As Measured by TGA Analysis under N_2 Stream[a]

	$T_{10\%}$ [°C]	$T_{50\%}$ [°C]	R_{780} [%]	T_{DTGmax} [°C]
P-lignin	284	711	48	334
ST-lignin	135	411	34	376
SM-lignin	227	434	40	313
SB-lignin	221	407	29	349
IT-lignin	189	558	37	342
IM-lignin	270	652	43	329
IB-lignin	240	576	35	320

[a] For comparison, data for the parent material (P-lignin) are also presented.

The char mass residue at 780 °C is found to decrease in all soluble fractions compared to P-lignin (48%), being maximum for SM-lignin (40%) followed by ST- (34%) and SB-lignin (29%). In applications where lignin is employed as bioderived carbon precursor, such as in the case of the preparation of carbon fibers, the possibility to control predictively the amount of char residue upon pyrolysis represents an important factor. In this respect, solvent fractionation may be used as a valuable tool to achieve this purpose. Accordingly, a potential correlation between char mass residue of P-lignin and all soluble fractions and their corresponding M_n value obtained by

GPC analysis was evaluated. As shown in Figure 7, the amount of char at 780 °C follows a linear regression with the molecular weight of the materials, with an excellent correlation factor R^2 of 0.99. These results indicate that the final mass residue upon pyrolysis may be fine-tuned by selective control of the molecular weight of lignin fractions via the simple selection of a suitable fractionation solvent.

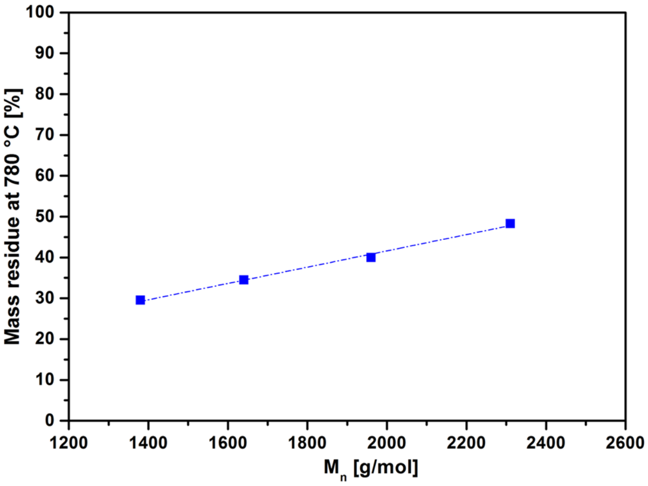

Figure 7. Final char residue at 780 °C as a function of M_n for P-lignin and for all soluble lignin fractions.

CONCLUSION

A straightforward fractionation approach was presented in this work aimed at obtaining readily usable lignin fractions with well-defined characteristics by appropriate selection of extracting solvent. This methodology separately employed tetrahydrofuran, methanol and 2-butanone to extract in a single-step soluble and insoluble fractions from a commercially available softwood kraft lignin. The fractionation yield was found to be highest for tetrahydrofuran, followed by methanol and then 2-butanone. These results evidenced that the amount of extracted fraction is primarily correlated with the Flory−Huggins polymer−solvent interaction parameter. However, the hydrogen bonding interactions between solvent and lignin were found to play a key role during the extraction process. Chemical characterization of the lignin fractions by means of FTIR spectroscopy revealed that the chemical composition of the extracted materials (soluble and insoluble) is highly dependent upon the chemical nature of the extraction solvent. In particular, the relative concentration of hydroxyl and carbonyl groups in the resulting fractions was found to be well correlated with the hydrogen bonding ability of the solvent (i.e., the hydrogen bonding contribution to the solubility parameter δ_h), being highest for methanol. These evidence were found to be in excellent agreement with the results obtained by means of quantitative ^{13}C NMR and UV−vis spectroscopy. GPC analysis on the soluble materials highlighted a decrease of molecular weight (and narrower molecular weight distribution) upon fractionation, with the lowest values of M_n and PDI found for the soluble material recovered after treatment with 2-butanone. In agreement with the previous results, this behavior was related to the poor hydrogen bonding ability of this solvent that limits the extraction to shorter macromolecular chains (as opposed to methanol that allowed us to dissolve efficiently significantly higher molecular weights). In addition, a linear correlation was found between the molecular weight of the fractionated materials and their T_g, based on the Flory−Fox model. Finally, TGA measurements were employed to evaluate the thermal stability of all extracted materials. In particular, in view of the use of lignin as bioderived carbon precursor (e.g., carbon fibers), a linear correlation was found between the char mass residue of pristine and soluble lignin fractions and their corresponding molecular weight. This behavior clearly indicates that a predictive fine-tuning of the final mass residue upon pyrolysis can be achieved by selective control of the molecular weight of lignin fractions through simple selection of a suitable fractionation solvent.

The results of this study give a clear demonstration of the direct correlation between the characteristics of the fractionation solvent and the properties of the extracted materials as predictive tool for the development of highly performing lignin-based systems.

ASSOCIATED CONTENT

Ⓢ Supporting Information

The Supporting Information is available free of charge on the ACS Publications website at DOI: 10.1021/acssuschemeng.5b01722.

> Differential thermal gravimetric analysis curves and related results of lignin fractions (soluble and insoluble) performed in air, ^{13}C NMR spectra of lignin fractions (PDF).

AUTHOR INFORMATION

Corresponding Author

*Gianmarco Griffini. Email: gianmarco.griffini@polimi.it. Tel: +39 022399 3213.

Notes

The authors declare no competing financial interest.

ACKNOWLEDGMENTS

This project was funded by the European Commission's Seventh Framework Programme for research, technological development and demonstration under grant agreement no FP7-KBBE-2013-7-613802 ("*ValorPlus - Valorisation of biorefinery by-products leading to closed loop systems with improved economic and environmental performance*"). Authors gratefully acknowledge Gigliola Clerici for support with GPC and thermal analysis. Prof. Andrea Mele, Prof. Paola D'Arrigo and their collaborators are acknowledged for assistance with ^{13}C NMR measurements.

REFERENCES

(1) *Report of the World Commission on Environment and Development: Our Common Future*; Annex to document A/42/427 - Development and International Co-operation: Environment; World Commission on Environment and Development (WCED): Oxford, United Kingdom, 1987; http://www.un-documents.net/ocf-02.htm#I.

(2) Ragauskas, A. J.; Beckham, G. T.; Biddy, M. J.; Chandra, R.; Chen, F.; Davis, M. F.; Davison, B. H.; Dixon, R. A.; Gilna, P.; Keller, M.; Langan, P.; Naskar, A. K.; Saddler, J. N.; Tschaplinski, T. J.; Tuskan, G. A.; Wyman, C. E. Lignin Valorization: Improving Lignin Processing in the Biorefinery. *Science* **2014**, *344* (6185), 1246843-1−1246843-10.

(3) Lora, J.; Glasser, W. Recent Industrial Applications of Lignin: A Sustainable Alternative to Nonrenewable Materials. *J. Polym. Environ.* **2002**, *10* (1−2), 39−48.

(4) Gellerstedt, G.; Henriksson, G. Lignins Major Sources, Structure and Properties. In *Monomers, Polymers and Composites from Renewable Resources*; Belgacem, M. N.; Gandini, A., Eds.; Elsevier: Amsterdam, The Netherlands, 2008; pp 201−224.

(5) Laurichesse, S.; Avérous, L. Chemical modification of lignins: Towards biobased polymers. *Prog. Polym. Sci.* **2014**, *39* (7), 1266−1290.

(6) Belgacem, M. N.; Blayo, A.; Gandini, A. Organosolv lignin as a filler in inks, varnishes and paints. *Ind. Crops Prod.* **2003**, *18* (2), 145−153.

(7) Lora, J. Industrial Commercial Lignins: Sources, Properties and Applications. In *Monomers, Polymers and Composites from Renewable Resources*; Belgacem, M. N.; Gandini, A., Eds.; Elsevier: Amsterdam, The Netherlands, 2008; pp 225−241.

(8) Doherty, W. O. S.; Mousavioun, P.; Fellows, C. M. Value-adding to cellulosic ethanol: Lignin polymers. *Ind. Crops Prod.* **2011**, *33* (2), 259−276.

(9) Gellerstedt, G. Softwood kraft lignin: Raw material for the future. *Ind. Crops Prod.* **2015**, *77*, 845−854.

(10) Duval, A.; Lawoko, M. A review on lignin-based polymeric, micro- and nano-structured materials. *React. Funct. Polym.* **2014**, *85* (0), 78−96.

(11) Gandini, A. Polymers from Renewable Resources: A Challenge for the Future of Macromolecular Materials. *Macromolecules* **2008**, *41* (24), 9491−9504.

(12) Gandini, A.; Belgacem, M. N. Lignins as Components of Macromolecular Materials. In *Monomers, Polymers and Composites from Renewable Resources*; Belgacem, M. N.; Gandini, A., Eds.; Elsevier: Amsterdam, The Netherlands, 2008; pp 243−271.

(13) Aracri, E.; Diaz Blanco, C.; Tzanov, T. An enzymatic approach to develop a lignin-based adhesive for wool floor coverings. *Green Chem.* **2014**, *16* (5), 2597−2603.

(14) Fox, S. C.; McDonald, A. G. Chemical and Thermal Characterization of Three Industrial Lignins and Their Corresponding Lignin Esters. *BioResources* **2010**, *5* (2), 990−1009.

(15) Li, H.; McDonald, A. G. Fractionation and characterization of industrial lignins. *Ind. Crops Prod.* **2014**, *62*, 67−76.

(16) Sivasankarapillai, G.; McDonald, A. G.; Li, H. Lignin valorization by forming toughened lignin-co-polymers: Development of hyperbranched prepolymers for cross-linking. *Biomass Bioenergy* **2012**, *47*, 99−108.

(17) Bouajila, J.; Dole, P.; Joly, C.; Limare, A. Some laws of a lignin plasticization. *J. Appl. Polym. Sci.* **2006**, *102* (2), 1445−1451.

(18) Helander, M.; Theliander, H.; Lawoko, M.; Henriksson, G.; Zhang, L.; Lindström, M. E. Fractionation of Technical Lignin: Molecular Mass and pH Effects. *BioResources* **2013**, *8* (2), 2270−2282.

(19) Alekhina, M.; Ershova, O.; Ebert, A.; Heikkinen, S.; Sixta, H. Softwood kraft lignin for value-added applications: Fractionation and structural characterization. *Ind. Crops Prod.* **2015**, *66*, 220−228.

(20) Sun, R.; Tomkinson, J.; Bolton, J. Effects of precipitation pH on the physico-chemical properties of the lignins isolated from the black liquor of oil palm empty fruit bunch fibre pulping. *Polym. Degrad. Stab.* **1999**, *63* (2), 195−200.

(21) García, A.; Toledano, A.; Serrano, L.; Egüés, I.; González, M.; Marín, F.; Labidi, J. Characterization of lignins obtained by selective precipitation. *Sep. Purif. Technol.* **2009**, *68* (2), 193−198.

(22) Colyar, K. R.; Pellegrino, J.; Kadam, K. Fractionation of Pre-Hydrolysis Products from Lignocellulosic Biomass by an Ultrafiltration Ceramic Tubular Membrane. *Sep. Sci. Technol.* **2008**, *43* (3), 447−476.

(23) Toledano, A.; Serrano, L.; Garcia, A.; Mondragon, I.; Labidi, J. Comparative study of lignin fractionation by ultrafiltration and selective precipitation. *Chem. Eng. J.* **2010**, *157* (1), 93−99.

(24) Dodd, A. P.; Kadla, J. F.; Straus, S. K. Characterization of Fractions Obtained from Two Industrial Softwood Kraft Lignins. *ACS Sustainable Chem. Eng.* **2015**, *3* (1), 103−110.

(25) Yuan, T.-Q.; He, J.; Xu, F.; Sun, R.-C. Fractionation and physico-chemical analysis of degraded lignins from the black liquor of Eucalyptus pellita KP-AQ pulping. *Polym. Degrad. Stab.* **2009**, *94* (7), 1142−1150.

(26) Arshanitsa, A.; Ponomarenko, J.; Dizhbite, T.; Andersone, A.; Gosselink, R. J. A.; van der Putten, J.; Lauberts, M.; Telysheva, G. Fractionation of technical lignins as a tool for improvement of their antioxidant properties. *J. Anal. Appl. Pyrolysis* **2013**, *103*, 78−85.

(27) Mörck, R.; Reimann, A.; Kringstad, K. P. Fractionation of Kraft Lignin by Successive Extraction with Organic Solvents. III. Fractionation of Kraft Lignin from Birch. *Holzforschung* **1988**, *42* (2), 111−116.

(28) Yoshida, H.; Mörck, R.; Kringstad, K. P.; Hatakeyama, H. Fractionation of Kraft Lignin by Successive Extraction with Organic Solvents. II. Thermal Properties of Kraft Lignin Fractions. *Holzforschung* **1987**, *41* (3), 171−176.

(29) Cui, C.; Sun, R.; Argyropoulos, D. S. Fractional Precipitation of Softwood Kraft Lignin: Isolation of Narrow Fractions Common to a Variety of Lignins. *ACS Sustainable Chem. Eng.* **2014**, *2* (4), 959−968.

(30) Ten, E.; Vermerris, W. Recent developments in polymers derived from industrial lignin. *J. Appl. Polym. Sci.* **2015**, *132* (24), 42069-1−42069-13.

(31) Sen, S.; Patil, S.; Argyropoulos, D. S. Thermal properties of lignin in copolymers, blends, and composites: a review. *Green Chem.* **2015**, *17* (11), 4862−4887.

(32) Cateto, C. A.; Barreiro, M. F.; Rodrigues, A. E.; Brochier-Salon, M. C.; Thielemans, W.; Belgacem, M. N. Lignins as macromonomers for polyurethane synthesis: A comparative study on hydroxyl group determination. *J. Appl. Polym. Sci.* **2008**, *109* (5), 3008−3017.

(33) Flory, P. J. Thermodynamics of High Polymer Solutions. *J. Chem. Phys.* **1941**, *9* (8), 660−660.

(34) Huggins, M. L. Solutions of Long Chain Compounds. *J. Chem. Phys.* **1941**, *9* (5), 440−440.

(35) Hansen, C. M. The Universality of the Solubility Parameter. *Ind. Eng. Chem. Prod. Res. Dev.* **1969**, *8* (1), 2−11.

(36) Vebber, G. C.; Pranke, P.; Pereira, C. N. Calculating hansen solubility parameters of polymers with genetic algorithms. *J. Appl. Polym. Sci.* **2014**, *131* (1), 39696-1−39696-12.

(37) VanKrevelen, D. W. *Properties of Polymers: Their Correlation with Chemical Structure; Their Numerical Estimation and Prediction from Additive Group Contributions*, Third Completely Revised ed.; Elsevier Scientific Publishing Company: Amsterdam, The Netherlands, 1990.

(38) Barton, A. F. M. *Handbook of Solubility Parameters and Other Coehsion Parameters*; CRC Press, Inc.: Boca Raton, FL, 1983.

(39) Thielemans, W.; Wool, R. P. Lignin Esters for Use in Unsaturated Thermosets:â€‰ Lignin Modification and Solubility Modeling. *Biomacromolecules* **2005**, *6* (4), 1895−1905.

(40) Calvo-Flores, F. G.; Dobado, J. A.; Isac-Garcia, J.; Martin-Martinez, F. J. *Lignin and Lignans as Renewable Raw Materials*; John Wiley and Sons, Ltd.: Chichester, United Kingdom, 2015.

(41) Faix, O. Fourier Transform Infrared Spectroscopy. In *Methods in Lignin Chemistry*; Lin, S. Y.; Dence, C. W., Eds.; Springer-Verlag: Heidelberg, Germany, 1992; pp 233−241.

(42) Griffini, G.; Passoni, V.; Suriano, R.; Levi, M.; Turri, S. Polyurethane Coatings Based on Chemically Unmodified Fractionated Lignin. *ACS Sustainable Chem. Eng.* **2015**, *3* (6), 1145−1154.

(43) Saito, T.; Perkins, J. H.; Vautard, F.; Meyer, H. M.; Messman, J. M.; Tolnai, B.; Naskar, A. K. Methanol Fractionation of Softwood Kraft Lignin: Impact on the Lignin Properties. *ChemSusChem* **2014**, *7* (1), 221−228.

(44) Wang, K.; Xu, F.; Sun, R. Molecular Characteristics of Kraft-AQ Pulping Lignin Fractionated by Sequential Organic Solvent Extraction. *Int. J. Mol. Sci.* **2010**, *11* (8), 2988−3001.

(45) Gärtner, A.; Gellerstedt, G.; Tamminen, T. Determination of phenolic hydroxyl groups in residual lignin using a modified UV-method. *Nord. Pulp Pap. Res. J.* **1999**, *14* (2), 163−170.

(46) Schuerch, C. The Solvent Properties of Liquids and Their Relation to the Solubility, Swelling, Isolation and Fractionation of Lignin. *J. Am. Chem. Soc.* **1952**, *74* (20), 5061−5067.

(47) McKenna, G. B. Glass Formation and Glassy Behavior. In *Comprehensive Polymer Science*; Allen, G.; Bevington, J. C.; Booth, C.; Price, C., Eds.; Pergamon Press plc: Oxford, United Kingdom, 1989; Vol. 2, pp 311−362.